AHSA1 promotes proliferation and EMT by regulating ERK/CALD1 axis in hepatocellular carcinoma

Jiakang Zhang
Southern Medical University
Zhixuan Ren
Southern Medical University
Zhenghui Song
Southern Medical University
Junhao Lin
Southern Medical University
Yue Luo
Southern Medical University
Xiaopei Zou
Southern Medical University
Yingying Pan
Southern Medical University
Na Qi
Southern Medical University
Aimin Li
Southern Medical University
Xinhui Liu (liuxinhui89@126.com)
Southern Medical University

Research Article

Keywords: Hepatocellular carcinoma, AHSA1, ERK1/2, CALD1

Posted Date: June 9th, 2022

DOI: https://doi.org/10.21203/rs.3.rs-1626018/v1

Abstract

Background

Hepatocellular carcinoma (HCC) is one of the major causes of cancer-related death worldwide. AHSA1 as a chaperone of HSP90 promotes the maturation, stability, and degradation of related cancer-promoting proteins. However, the regulatory mechanism and biological function of AHSA1 in HCC are largely unknown. The purpose of this study is to elaborate the role of AHSA1 in HCC development.

Methods

Real-Time PCR, Western blotting, and Immunohistochemistry were used to determine the mRNA and protein expression of AHSA1 in liver epithelial cells, HCC cells, and tissues. Furthermore, both in vitro and in vivo, gain- and loss-of-function studies demonstrated the role of AHSA1 in the proliferation, invasion, metastasis, and epithelial-mesenchymal transition of HCC. To explore the molecular mechanism of AHSA1 in HCC, Western blotting, coimmunoprecipitation assay, and mass spectrometer assay were performed.

Results

Actually, we found AHSA1 was significantly upregulated in HCC tissues and cell lines, and was correlated with the poor prognosis of HCC patients. Furthermore, both in vitro and in vivo, gain- and loss-of-function studies demonstrated AHSA1 promoted the proliferation, invasion, metastasis, and epithelial-mesenchymal transition (EMT) of HCC. Moreover, the mechanistic study indicated that AHSA1 recruited ERK1/2 and promoted the phosphorylation and inactivation of CALD1, while ERK1/2 phosphorylation inhibitor, SCH772984, reversed the role of AHSA1 in the proliferation and EMT of HCC. Furthermore, we demonstrated the knockdown of CALD1 reversed the inhibition of proliferation and EMT by knocking AHSA1 in HCC. We also illustrated a new molecular mechanism associated with AHSA1 in HCC that was independent of HSP90 and MEK1/2.

Conclusions

In summary, AHSA1 may play an oncogenic role in HCC by regulating ERK/CALD1 axis and serve as a novel therapeutic target for HCC.

1. Introduction

Primary liver cancer is one of the primary causes of cancer-related death worldwide. Hepatocellular carcinoma (HCC) is the most common type of primary liver cancer, risk factors of which include hepatitis B virus (HBV) infection, hepatitis C virus (HCV) infection, alcohol abuse, and so on[1]. Since most of HCC

patients were diagnosed in advanced stage and therapeutic strategies are limited, the 5-year survival rate of HCC is still under 20%[2]. Targeted therapy, as a vital way for advanced HCC patients, includes Lenvatinib and Sorafenib[3–5]. However, the clinical efficacy of current therapies is still not satisfactory for HCC patients. Thus, it remains critical to understand the molecular mechanism and identify therapeutic targets for HCC.

The activator of 90kDa heat shock protein ATPase homolog 1 (AHSA1) was reported to play a role in the regulation of related cancer-promoting proteins [6–9] depending on a chain reaction between the central region of HSP90 and the AHSA1 N-terminal domain [10]. Recently, AHSA1 has been found to play an oncogenic role by promoting the proliferation and metastasis of malignant tumors including osteosarcoma, colorectal adenocarcinoma, and multiple myeloma[11–13]. However, the functional role and underlying mechanism of AHSA1 in the occurrence and development of HCC have not yet been characterized.

In a brief, by detecting the expression of AHSA1 in the HCC public database and tissue, we identified AHSA1 was significantly upregulated in HCC tissues and positively correlated with a higher rate of recurrence and poor prognosis in HCC patients. Furthermore, both in vitro and in vivo, gain- and loss-of-function studies demonstrated that AHSA1 promoted the proliferation, invasion, metastasis, and epithelial-mesenchymal transition (EMT) of HCC. Moreover, the mechanistic study indicated that AHSA1 recruited ERK1/2 and promoted the phosphorylation and inactivation of CALD1, while ERK1/2 phosphorylation inhibitor, SCH772984, reversed the role of AHSA1 in the proliferation and EMT of HCC. Furthermore, we demonstrated that the knockdown of CALD1 reversed the inhibition of proliferation and EMT by knocking AHSA1 in HCC. Surprisingly, We also illustrated a new molecular mechanism associated with AHSA1 in HCC that was independent of HSP90 and MEK1/2. Overall, this study describes a novel carcinogenic role of AHSA1 in HCC and provides a new direction for HCC treatment.

2. Materials And Methods

2.1 Bioinformatics analysis

Data, required for bioinformatics analysis, were downloaded from the GEO (GSE14520 and GSE50579) and TCGA-LIHC databases. R software (version 3.5.1) and its packages were employed to analyze these data. AHSA1-related genes ($|R > 0.5|$, $p < 0.001$) in TCGA-LIHC were identified and used for functional and pathway enrichment analyses including the Kyoto Encyclopedia of Genes and Genomes (KEGG) pathway and Gene Ontology (GO).

2.2 Antibodies

AHSA1, N-cadherin, 6-his, vimentin, HSP90, MEK1/2, E-cadherin, and CALD1 antibodies were obtained from Proteintech (Wuhan, China). ERK1/2, Phospho-MEK1/2, and Phospho-ERK1/2 antibodies were obtained from Cell Signaling Technology (Beverly, Massachusetts, USA). Ki67 antibody was obtained from Abcam (Cambridge, Massachusetts, USA). Phospho-CALD1 antibody was purchased from Thermo

Fisher Scientific (Waltham, MA, USA). β-tubulin antibody was obtained from Bioworld Technology (Bloomington, MN, USA).

2.3 Cell culture and transfection

The HCC cell lines, PLC/PRF/5, HCCLM3, Huh-7, Hep3B, and HepG2, and the control liver epithelial cell line, LO2, were purchased from Zhong Qiao Xin Zhou Biotechnology (Shanghai, China). The cells were inoculated into culture dishes purchased from Guangzhou Jet Biofiltration (Guangzhou, China) and added to Dulbecco's Modified Eagle's Medium (DMEM) containing 10% fetal bovine serum to maintain growth. The growth environment temperature was maintained at 37°C with 5% CO_2. The overexpression plasmid pcDNA3.1-AHSA1, empty vector pcDNA3.1, shRNAs targeting AHSA1, and sh-control were purchased from OBiO Technology (Shanghai, China). The sequences of shRNAs targeting AHSA1 and sh-control were as follows: sh-AHSA1-1, GCATGATCTTACCTACAAT; sh-AHSA1-2, CCATCACCTTGACCTTCAT; sh-control, CCTAAGGTTAAGTCGCCCTCG. The siRNAs targeting CALD1 and si-NC were obtained from RIBOBIO (Guangzhou, China). The sequences of siRNAs targeting CALD1 were as follows: si-CALD1-1, AGAGCTTCATGGATCGAAA; si-CALD1-2, GTACGCAACATCAAG AGTA; si-CALD1-3, GAAGGAGTTCGACCCAACA. Lipofectamine 3000 (Thermo Scientific, Waltham, MA, USA) was used for conventional cell transfection for 72 h. AHSA1 expression was detected by western blotting.

2.4 Immunohistochemistry (IHC)

Referring to the manufacturer’s instructions, the IHC detection kit (PV-9000)(ZsBio, Beijing, China), was used to assess the expression of AHSA1 in the HCC tissue arrays (HLivH180Su15)(Shanghai Outdo Biotech Company, Shanghai, China). The IHC score was obtained by determining the intensity of staining and the positive area (intensity score + area score) and described by the following rules: scores between 0 and 6 represented low expression, and those > 6 were considered high expression.

2.5 Total RNA extraction and Real-Time PCR

By means of the total RNA isolation kit (Foregene, Chengdu, China) and the PrimeScript RT kit (Takara Biomedical Technology, Beijing, China), RNA was extracted from the cells and reverse transcribed into DNA. Referring to the operation manual of the LightCycler480 system (Roche, Basel, Switzerland), DNA was added into the 8-tube system containing primers and TB Green Premix Ex TaqII(Takara Biomedical Technology, Beijing, China) to conduct Real-Time PCR. DNA expression was standardized to the expression of β-actin, and the relative expression level was calculated using $2-\Delta\Delta Ct$. The primer sequences included: AHSA1: (forward) 5'-GGCACTAAGCGGTCCTGAG-3', (reverse) 5'-CTCCACT TCATCCACGCTGT-3'; β-actin: (forward) 5'-AGAAGGATTCCTATGG GCGAC-3', and (reverse) 5'–AGTACTTGCGCTCA GGAGGA-3 '.

2.6 Western blotting, coimmunoprecipitation (Co-IP) assay, and mass spectrometer (MS) assay

In a brief, protein samples were separated on 10% pre-gel and transferred to a polyvinylidene fluoride(PVDF) membrane. Via using 5% BSA at 37°C for 1 h, the bands were blocked and incubated with

a primary antibody at 37°C for 2h. After 3 cleanings through using TBST, the band was incubated with a secondary antibody on a shaker at 37°C for 1.5 h. Via the MiniChemi chemiluminescence imaging and analysis system (Sage Creation Science, Beijing, China), the special protein bands of the membrane became visible on the computer screen after spraying enhanced chemiluminescence reagents from Millipore (Billerica, MA, USA). HCC cell protein samples were coimmunoprecipitated using the Pierce Co-IP kit (Thermo Scientific, Waltham, MA, USA), and the target protein that corresponded to the cured antibody and its stable binding protein were obtained, and the final special protein samples were analyzed by Western blotting. For the MS assay, the protein sample obtained from the Co-IP experiment contained proteins interacting with AHSA1, and 8M urea was used to supplement the volume of the protein sample to 200ul. Next, the sample was added with a final concentration of 2mM DTT, reacted in an incubator at 56 ℃ for 30 min, and cooled to room temperature. The sample was added with a final concentration of 10mM IAA and reacted at room temperature for 30 min. Then, the sample was added to a 10KD protein ultrafiltration tube and centrifuged (14000g, 30min), washed three times by using ammonium bicarbonate solution, and then digested by trypsin (37 ℃, 12 hours). Finally, the sample was washed with water for mass spectrometry, centrifuged (14000g, 20min), dried, and analyzed by one mass spectrometer (Thermo Scientific™ Orbitrap Fusion™ Tribrid™, American). The original data was compared with the data in the UniProt database.

2.7 EdU assay

An EdU proliferation test was conducted using the in vitro Cell-Light EdU Apollo 567 imaging kit (RiboBio, Guangzhou, China). In brief, after transfection with a plasmid for 72 h or transduction with lentivirus, HCC cells were seeded in 96-well plates (2x104 cells/well) and stained with EdU. The figures of EdU positive cells (red) in three random observation fields were captured via an inverted fluorescence microscope (Olympus, Beijing, China).

2.8 Clone formation experiment

Cell population dependence and proliferation were evaluated using a cell cloning experiment. In brief, cells, HepG2 and HCCLM3, receiving transduction of AHSA1 knock-down lentivirus or control lentivirus, were evenly distributed at the bottom of 6-well plates (500 cells/well). After the cells were incubated for three weeks. The cells were then infiltrated with paraformaldehyde for 60 min and stained with crystal violet (0.1% methanol) for 20 min. Finally, the number of clones was calculated.

2.9 Cell Counting Kit 8 (CCK-8) assay

Hep3B cells were evenly inoculated in 96-well plates (2,000 cells/well), and the corresponding SCH772984 (Selleck Chemicals, Shanghai, China) was added via the concentration gradient. CCK-8 (Dojindo Laboratories, Mashikimachi, Japan) was used two hours before and the absorbance of the sample in the hole at 450 nm was measured at 24, 48, and 72 h.

2.10 Cell wound healing, migration, and invasion assays

To conduct the cell wound healing test, cells were added to a six-well plate, the tip of a 1 ml pipette was used to make scratches, and cell migration across the gaps was observed via a microscope at 0, 24, 48, and 72 h. For the Transwell experiment, the suspended cells in DMEM without serum were inoculated in the chamber (the aperture of the basement membrane was 8.0 mm, 1×105 cells/chamber), and placed in a 24-well plate. The corresponding wells were supplemented with DMEM containing 20% serum and incubated for 24 h. Cells were removed which did not enter the basement membrane, and the membrane was placed in paraformaldehyde for cell immobilization. The membrane was then dyed with crystal violet solution (0.1% methanol) for 20 min. Positive cells on the membrane (purple) were counted using three fields of vision. For the invasion experiment, a matrix gel (Corning, China) was diluted referring to the manufacturer's instructions, and evenly spread on the surface of the membrane. Cells, suspended in DMEM without serum, were inoculated in the chamber (the aperture of the basement membrane was 8.0 mm, 1x105 cells/chamber), and placed in a 24-well plate. DMEM with 20% serum was supplemented to the corresponding well of each chamber. After 24 h, Cells were removed which did not enter the basement membrane, and the membrane was placed in paraformaldehyde for cell immobilization. The membrane was then dyed in crystal violet solution (0.1% methanol) for 20 min. Positive cells on the membrane (purple) were counted using three fields of vision.

2.11 Subcutaneous model of nude mice

According to the international animal care and maintenance regulations, the mouse experiment was conducted and was approved by the Experimental Animal Ethics Committee, Guilin Medical University. In short, 2.5×106 HCCLM3 cells with knocked-down AHSA1 or control lentivirus were used to inject into the posterior right lateral thigh of nude mice(male, bodyweight: ~19 g, 6 weeks) (Hunan SJA laboratory animals, Hunan, China). The mice were euthanized on day 17 to evaluate tumor size. All tumor tissues were observed and photographed through a microscope (Olympus, Beijing, China). Each tumor tissue specimen was then fixed with formalin, embedded in paraffin, and H&E and HRP-DAB immunohistochemical staining were performed.

2.12 Nude mouse lung metastasis model

In brief, 1×106 cells/80μl AHSA1 knock-down or empty vector control HCCLM3 cells were intravenously injected into the tail vein of nude mice. Lung metastasis model mice were euthanized on day 58 to evaluate the number of tumors. All lung tissues were observed and photographed through a microscope (Olympus, Beijing, China). Each lung tissue specimen was fixed with formalin, embedded in paraffin, and H&E and HRP-DAB immunohistochemical staining were performed.

2.13 Statistical analysis

Student T-tests were used for analysis. The relationship between AHSA1 expression and patient clinical and prognostic characteristics was analyzed by χ^2 or Fisher's exact tests. OS and DFS were calculated by log-rank test. All statistical results are expressed as the mean ± standard error by GraphPad Prism6 (San Diego, CA, USA) and met the conditions of a bilateral test. Each non-animal experiment was repeated in three independent experiments.

3. Results

3.1 AHSA1 was upregulated and predicted a poor prognosis of HCC.

To explore the role of AHSA1 in HCC development, we first detected the expression of AHSA1 in TCGA-LIHC, GSE14520, and GSE50579 HCC databases[14]. As shown in Fig. 1A, AHSA1 was significantly upregulated in HCC cancerous tissues compared to adjacent tissues. Moreover, HCC patients with high-expression of AHSA1 had shorter overall survival (OS) and disease-free survival (DFS) than those with low-expression of AHSA1 (Fig. 1B). Furthermore, the basic expression levels of AHSA1 in HCC cell lines were higher than that in the normal cell line LO2 which were detected by quantitative real-time PCR and Western blot (Fig. 1C and S1A). To confirm the protein level of AHSA1 in HCC, IHC was used in the HCC microarray including 90 HCC paired tissues. Consistently, AHSA1 expression was significantly higher in HCC tissues than in adjacent tissues ($P < 0.001$, Fig. 1D -E). Subsequently, the potential association between AHSA1 and HCC patients' clinicopathological features was explored to understand the significance of AHSA1 in HCC. Notably, AHSA1 expression was positively correlated with HCC recurrence ($P < 0.001$, Table. S1).

3.2 AHSA1 promoted the proliferation of HCC both in vitro and in vivo.

To assess the role of AHSA1 in HCC, AHSA1 was knocked down in HepG2 and HCCLM3 cells using lentiviral transduction and overexpressed in Huh-7 and Hep3B cells. Transfection efficiency was determined by Western blotting (Fig. 2A). EdU analysis showed that knockdown of AHSA1 significantly inhibited cell proliferation ability in HepG2 and HCCLM3 cells compared to control cells. Moreover, the cell proliferation ability of Hep3B and Huh-7 cells were significantly upregulated by overexpression of AHSA1 (Fig. 2B-C). Consistently, the results of the clone formation experiment indicated that proliferation was obviously reduced in HepG2 and HCCLM3 cells after being transfected with sh-AHSA1-1 compared to the control group ($P < 0.05$, Fig. 2D-E).

A nude mouse subcutaneous tumor model was used to further analyze the effect of AHSA1 on the proliferation of HCC in vivo. HCCLM3 cells transfected with AHSA1 knock-down lentivirus or control lentivirus were injected into the skin of the right posterolateral thigh of male nude mice. As shown in Fig. 2F-G and S1B, a significant reduction of the tumor was found in mice injected with HCCLM3-sh-AHSA1-1, compared with those injected with HCCLM3-sh-control cells ($P < 0.001$). Furthermore, a reduction of Ki67 expression was observed in the HCCLM3-sh-AHSA1-1 group than HCCLM3-sh-control group by employing IHC staining (Fig. 2H). Interestingly, the expression of E-cadherin expression was

upregulated in the tumor of the HCCLM3-sh-AHSA1-1 group. Overall, AHSA1 upregulated the proliferation ability of HCC both in vitro and in vivo.

3.3 AHSA1 promoted the invasion, migration, and EMT of HCC both in vitro and in vivo.

Previous studies have shown that high AHSA1 expression is related to the occurrence of metastases[15] and the E-cadherin expression was upregulated by knockdown AHSA1 in vivo. We further explore the influence of AHSA1 on HCC cell migration, and invasion by employing transwell invasion, migration and wound healing, assays. The results showed that cell invasion and migration were significantly inhibited sh-AHSA1-1 group compared with the control group in both HepG2 and HCCLM3 cells while overexpression of AHSA1 significantly promotes Hep3B and Huh-7 cells invasion and migration (Fig. 3A-B and S1C-D). Consistently, a shorter healing distance was detected in the sh-AHSA1-1 group compared with the control group while reinforcement of cell healing was observed following AHSA1 overexpression (Fig. 3C-D). These results indicated that AHSA1 has a positive effect on cell invasion and migration of HCC.

To ascertain whether AHSA1 knock-down affects tumor metastasis in vivo, HCCLM3 cells transfected with AHSA1 knock-down lentivirus or control lentivirus were intravenously injected into 6-week-old male nude mice via tail vein. All mice were euthanized after 58 days to analyze the effect of AHSA1 on tumor cell migration. As shown in Fig. 3E-F, there were significantly fewer fluorescent tumor nodules in the lungs of mice injected with HCCLM3-sh-AHSA1-1, compared with those injected with HCCLM3-sh-control cells ($P < 0.001$). In addition, N-cadherin was downregulated and E-cadherin was upregulated in tumor tissues of mice injected with HCCLM3-sh-AHSA1-1, suggesting that loss of AHSA1 reduced the EMT of HCC in vivo (Fig. 3G). Thus, AHSA1 promoted cell migration and invasion ability of HCC in vitro and in vivo.

3.4 AHSA1 promoted the phosphorylation and inactivation of CALD1 by phosphorylation of ERK1/2.

Additional experiments were determined to explore the molecular mechanism of AHSA1 in HCC. Notably, overexpression of AHSA1 promoted the EMT of Hep3B and Huh-7 by upregulating the mesenchymal markers, N-cadherin and vimentin, and downregulating the epithelial marker, E-cadherin while knockdown of AHSA1 played an opposite effect on HepG2 and HCCLM3 cells (Fig. 4A). In addition, AHSA1-related genes detected in the TCGA-LIHC database were employed in KEGG and GO enrichment analysis. Through bioinformatic analysis, we found AHSA1-related genes were predominantly enriched in cell cycle, Spliceosome, and DNA replication (Fig. S1E). Moreover, the Co-IP protein sample solution was pulled down by AHSA1 antibody through protein Co-IP and assessed by qualitative mass spectrometry to determine the interaction protein of AHSA1 in HCC. As shown in Fig. 4B, sixteen proteins were strongly correlated with AHSA1, of which MAPK1 (ERK1/2) and its downstream target CALD1 were particularly noteworthy [16, 17]. Next, Co-IP was used to verify the interaction between AHSA1, CALD1, and ERK1/2 in Hep3B and Huh-7 cells (Fig. 4C and S2A). Furthermore, knockdown of AHSA1 promoted the protein level of CALD1 in HCCLM3 while overexpression of AHSA1 played a reverse effect on Hep3B cells (Fig. 4D). Prior studies have reported that phosphorylated ERK1/2 promoted CALD1 phosphorylation and inactivation. As shown in Fig. 4D, knockdown of AHSA1 inhibited CALD1 phosphorylation at Ser759 and ERK1/2 phosphorylation at Thr202/Tyr204 while overexpression of AHSA1 played a reverse effect on

Hep3B cells. Taken together, these results suggested that AHSA1 might promote phosphorylation of CALD1 at Ser759, and reduce CALD1 activity (in its non-phosphorylated form) by inducing phosphorylation of ERK1/2 at Thr202/Tyr204. In addition, we detected that CALD1 expression was significantly lower in HCC tissues and cell lines (Fig. 4E, 4F, and S2B). Interestingly, the molecular mechanism associated with AHSA1 in HCC cells was independent of HSP90 and MEK1/2 (Fig. S2C and S2D).

3.5 ERK1/2 phosphorylation inhibitor reversed the proliferation and EMT of HCC that was promoted by AHSA1 overexpression.

To verify the effect of ERK1/2 on the promotion of proliferation and EMT by AHSA1 in HCC, rescue experiments were performed with an ERK1/2 phosphorylation inhibitor, SCH772984. Prior studies set forth that SCH772984 inhibits the phosphorylation of residues in the ERK self-activation ring [18]. Within a certain range, CCK-8 results showed that as the concentration of SCH772984 increased, its effect on the survival of Hep3B cells was negligible (Fig. S2E). Based on the drug manufacturer's instructions and related literature reports[18], 4, 40, and 80 nM doses of SCH772984 were used, and as expected, ERK1/2 phosphorylation decreased after SCH772984 treatment (Fig. 5A). 40nM doses of SCH772984d as the effective concentration were used for further rescue assays. Using EdU assay, we found that overexpression of AHSA1 significantly promoted HCC proliferation which could be reversed by SCH772984(Fig. 5B-5C). Subsequent transwell and wound healing tests assays revealed that overexpression of AHSA1 led to an increase in HCC migration, which could be reversed by SCH772984(Fig. 5D-5G). In addition, the EMT and CALD1 regulated by AHSA1 overexpression were also reversed after treatment with SCH772984 (Fig. 5H). Taken together, SCH772984, as the ERK1/2 phosphorylation inhibitor, abrogated AHSA1-induced HCC proliferation and migration.

3.6 Inhibition of CALD1 reversed the inhibition of cell proliferation and EMT in HCC by knockdown of AHSA1.

To verify whether CALD1 may affect the oncogene role of AHSA1 in HCC, functional rescue experiments were performed. Inhibition of CALD1 expression by siRNA was then used and evidence of the knock-down efficiency of CALD1in HCCLM3 cells was offered by Western blot analysis(Fig. 6A). Using EdU assay, we found that knockdown of AHSA1 significantly inhibited HCC proliferation which could be reversed by CALD1 silencing(Fig. 6B-5C). Subsequent transwell and wound healing tests assays revealed that knockdown of AHSA1 led to decreased of HCC migration, which could be reversed by CALD1 silencing (Fig. 6D-5G). Moreover, the EMT and CALD1 regulated by AHSA1 overexpression were also reversed after the knockdown of CALD1 (Fig. 6H). Therefore, we conclude that CALD1 is required for AHSA1-induced HCC proliferation and EMT.

4. Discussion

Many HSP90 downstream proteins and molecular chaperones play a key role in cancer pathogenesis, suggesting that HSP90 is critical for an effective response to cancer treatment [19]. Actually, clinical trials

by means of some HSP90 inhibitors have stopped as a result of serious side effects such as ototoxicity and hepatotoxicity or stalled owing to therapy effects lower than expected [20, 21]. HSP90, an important molecule for cellular processes, was suppressed with severe consequences, emphasizing the value of further expounding the molecular chaperone mechanism of HSP90. AHSA1, one of the most active chaperones of HSP90, stimulated HSP90 ATPase activity to stabilize and strengthen the function of downstream target proteins[22]. However, the mechanism of AHSA1 in HCC has remained largely unexplored. This study correlated AHSA1 overexpression with poor survival prognosis in HCC patients and demonstrated that AHSA1 promoted the proliferation, invasion, metastasis, and EMT of HCC both in vitro and in vivo, and suggested that AHSA1 may be a carcinogenic gene in HCC.

EMT plays a critical role in proembryo formation, adult wound healing, and the development of many types of cancer. Indeed, tumor cells with EMT properties are important to cancer development[23]. This study showed that knocking down AHSA1 in two typical HCC cell lines, HepG2 and HCCLM3 resulted in downregulation of the mesenchymal markers, N-cadherin and vimentin, and the upregulation of the epithelial marker, E-cadherin. When AHSA1 expression was increased after plasmid transfection in Hep3B and Huh-7 cells, the results of the loss of E-cadherin and upregulation of N-cadherin and vimentin were obtained. These findings indicated that AHSA1 could promote the epithelial to mesenchymal transformation in HCC.

Surprisingly, we demonstrated AHSA1 recruited ERK1/2 and CALD1 and promoted ERK1/2 phosphorylation at Thr202/Tyr204, thereby increasing CALD1 phosphorylation at Ser759, causing CALD1 to lose its ability to inhibit ATPase activity and actin filament movement, ultimately increasing cell migration[24, 25]. An initial rescue experiment showed that AHSA1-induced ERK1/2 phosphorylation and subsequent EMT and HCC cell proliferation were prevented by the ERK1/2 phosphorylation inhibitor, SCH772984. A second rescue experiment, using a siRNA-mediated gene knock-down technique to inhibit CALD1 expression, was designed to verify whether knocking down AHSA1 inhibited EMT and HCC cell proliferation by increasing the functional (non-phosphorylated) form of CALD1. In short, AHSA1 further targeted CALD1 and promoted its phosphorylation by increasing the phosphorylation of ERK1/2 and enhancing EMT and HCC cell proliferation. Actually, these results are supported by previous findings that CALD1 inhibits cancer cell metastasis[26, 27]. Interestingly, the molecular mechanism of AHSA1 in HCC cells was independent of HSP90 and MEK1/2. Overall, this study showed that AHSA1, an important target for HCC treatment, is overexpressed in HCC patients and is associated with a poor prognosis. In fact, the oral ERK1/2 phosphorylation inhibitor, MK-8353, which has a similar mechanism to the ERK1/2 phosphorylation inhibitor, SCH772984, has shown some promising results in clinical studies of cancer patients[28], implies a new choice for patients with AHSA1 overexpression. Additional clinical trials should be considered to assess patient sensitivity to MK-8353 when the AHSA1 of the patient is overexpressed.

5. Conclusion

In summary, this study showed that AHSA1 increased phosphorylation of ERK1/2 and prevented CALD1 activity, ultimately enhancing EMT and HCC cell proliferation. AHSA1 may function as an effective diagnostic and prognostic biomarker for HCC patients.

Abbreviations

HCC	Hepatocellular carcinoma
EMT	epithelial-mesenchymal transition
HBV	hepatitis B virus
HCV	hepatitis C virus
AHSA1	activator of 90kDa heat shock protein ATPase homolog 1
KEGG	Kyoto Encyclopedia of Genes and Genomes
DMEM	Dulbecco's Modified Eagle's Medium
IHC	Immunohistochemistry
Co-IP	Coimmunoprecipitation
MS	mass spectrometer
PVDF	polyvinylidene fluoride
OS	overall survival
DFS	disease-free survival
LO2	normal immortalized hepatic epithelial cell

Declaration

Ethics approval and consent to participate

According to the international animal care and maintenance regulations, the mouse experiment was conducted and was approved by the Experimental Animal Ethics Committee, Guilin Medical University.

Consent for publication

Consent for publication was obtained from every patient.

Availability of data and materials

All data generated or analysed during this study are included in this published article and its Additional files.

Competing interests

All co-authors had no conflicts of interest to disclose.

Funding

This work was supported by the National Natural Science Foundation of China (NO.81874173); Science and Technology Program of Guangzhou, China (NO.202102020098, NO.202002030075); President's fund of Integrated hospital of traditional Chinese Medicine (NO.20203006).

Authors' contributions

XL and AL contributed to the concept and design of the study. JZ and ZR performed experiments and wrote the manuscript. ZS, XZ, and NQ carried out the bioinformatic analysis. JL, YL, and YP are responsible for the statistical analysis. All authors read and approved the final manuscript.

Acknowledgements

Not applicable.

References

1. A. Huang, X.R. Yang, W.Y. Chung, A.R. Dennison, J. Zhou, Targeted therapy for hepatocellular carcinoma, Signal Transduct Target Ther, 5 (2020) 146.
2. J.D. Yang, P. Hainaut, G.J. Gores, A. Amadou, A. Plymoth, L.R. Roberts, A global view of hepatocellular carcinoma: trends, risk, prevention and management, Nat Rev Gastroenterol Hepatol, 16 (2019) 589-604.
3. Z.T. Al-Salama, Y.Y. Syed, L.J. Scott, Lenvatinib: A Review in Hepatocellular Carcinoma, Drugs, 79 (2019) 665-674.
4. Z. Cheng, J. Wei-Qi, D. Jin, New insights on sorafenib resistance in liver cancer with correlation of individualized therapy, Biochim Biophys Acta Rev Cancer, 1874 (2020) 188382.
5. A.L. Cheng, Y.K. Kang, Z. Chen, C.J. Tsao, S. Qin, J.S. Kim, R. Luo, J. Feng, S. Ye, T.S. Yang, J. Xu, Y. Sun, H. Liang, J. Liu, J. Wang, W.Y. Tak, H. Pan, K. Burock, J. Zou, D. Voliotis, Z. Guan, Efficacy and safety of sorafenib in patients in the Asia-Pacific region with advanced hepatocellular carcinoma: a phase III randomised, double-blind, placebo-controlled trial, Lancet Oncol, 10 (2009) 25-34.
6. G.P. Lotz, H. Lin, A. Harst, W.M. Obermann, Aha1 binds to the middle domain of Hsp90, contributes to client protein activation, and stimulates the ATPase activity of the molecular chaperone, J Biol Chem, 278 (2003) 17228-17235.
7. L. Sun, T. Prince, J.R. Manjarrez, B.T. Scroggins, R.L. Matts, Characterization of the interaction of Aha1 with components of the Hsp90 chaperone machine and client proteins, Biochim Biophys Acta, 1823 (2012) 1092-1101.
8. D.M. Dunn, M.R. Woodford, A.W. Truman, S.M. Jensen, J. Schulman, T. Caza, T.C. Remillard, D. Loiselle, D. Wolfgeher, B.S. Blagg, L. Franco, T.A. Haystead, S. Daturpalli, M.P. Mayer, J.B. Trepel, R.M.

Morgan, C. Prodromou, S.J. Kron, B. Panaretou, W.G. Stetler-Stevenson, S.K. Landas, L. Neckers, G. Bratslavsky, D. Bourboulia, M. Mollapour, c-Abl Mediated Tyrosine Phosphorylation of Aha1 Activates Its Co-chaperone Function in Cancer Cells, Cell Rep, 12 (2015) 1006-1018.

9. W. Xu, K. Beebe, J.D. Chavez, M. Boysen, Y. Lu, A.D. Zuehlke, D. Keramisanou, J.B. Trepel, C. Prodromou, M.P. Mayer, J.E. Bruce, I. Gelis, L. Neckers, Hsp90 middle domain phosphorylation initiates a complex conformational program to recruit the ATPase-stimulating cochaperone Aha1, Nat Commun, 10 (2019) 2574.
10. P. Meyer, C. Prodromou, C. Liao, B. Hu, S.M. Roe, C.K. Vaughan, I. Vlasic, B. Panaretou, P.W. Piper, L.H. Pearl, Structural basis for recruitment of the ATPase activator Aha1 to the Hsp90 chaperone machinery, Embo j, 23 (2004) 1402-1410.
11. D. Zheng, W. Liu, W. Xie, G. Huang, Q. Jiang, Y. Yang, J. Huang, Z. Xing, M. Yuan, M. Wei, Y. Li, J. Yin, J. Shen, Z. Shi, AHA1 upregulates IDH1 and metabolic activity to promote growth and metastasis and predicts prognosis in osteosarcoma, Signal Transduct Target Ther, 6 (2021) 25.
12. D. Kim, J.W. Moon, D.H. Min, E.S. Ko, B. Ahn, E.S. Kim, J.Y. Lee, AHA1 regulates cell migration and invasion via the EMT pathway in colorectal adenocarcinomas, Sci Rep, 11 (2021) 19946.
13. C. Gu, Y. Wang, L. Zhang, L. Qiao, S. Sun, M. Shao, X. Tang, P. Ding, C. Tang, Y. Cao, Y. Zhou, M. Guo, R. Wei, N. Li, Y. Xiao, J. Duan, Y. Yang, AHSA1 is a promising therapeutic target for cellular proliferation and proteasome inhibitor resistance in multiple myeloma, J Exp Clin Cancer Res, 41 (2022) 11.
14. Z. Tang, C. Li, B. Kang, G. Gao, C. Li, Z. Zhang, GEPIA: a web server for cancer and normal gene expression profiling and interactive analyses, Nucleic Acids Res, 45 (2017) W98-W102.
15. R. Cao, J. Shao, Y. Hu, L. Wang, Z. Li, G. Sun, X. Gao, microRNA-338-3p inhibits proliferation, migration, invasion, and EMT in osteosarcoma cells by targeting activator of 90 kDa heat shock protein ATPase homolog 1, Cancer Cell Int, 18 (2018) 49.
16. C.M. Hai, Z. Gu, Caldesmon phosphorylation in actin cytoskeletal remodeling, Eur J Cell Biol, 85 (2006) 305-309.
17. J. Kordowska, R. Huang, C.L. Wang, Phosphorylation of caldesmon during smooth muscle contraction and cell migration or proliferation, J Biomed Sci, 13 (2006) 159-172.
18. E.J. Morris, S. Jha, C.R. Restaino, P. Dayananth, H. Zhu, A. Cooper, D. Carr, Y. Deng, W. Jin, S. Black, B. Long, J. Liu, E. Dinunzio, W. Windsor, R. Zhang, S. Zhao, M.H. Angagaw, E.M. Pinheiro, J. Desai, L. Xiao, G. Shipps, A. Hruza, J. Wang, J. Kelly, S. Paliwal, X. Gao, B.S. Babu, L. Zhu, P. Daublain, L. Zhang, B.A. Lutterbach, M.R. Pelletier, U. Philippar, P. Siliphaivanh, D. Witter, P. Kirschmeier, W.R. Bishop, D. Hicklin, D.G. Gilliland, L. Jayaraman, L. Zawel, S. Fawell, A.A. Samatar, Discovery of a novel ERK inhibitor with activity in models of acquired resistance to BRAF and MEK inhibitors, Cancer Discov, 3 (2013) 742-750.
19. M. Nouri-Vaskeh, L. Alizadeh, K. Hajiasgharzadeh, A. Mokhtarzadeh, M. Halimi, B. Baradaran, The role of HSP90 molecular chaperones in hepatocellular carcinoma, J Cell Physiol, 235 (2020) 9110-9120.

20. S. Yang, H. Xiao, L. Cao, Recent advances in heat shock proteins in cancer diagnosis, prognosis, metabolism and treatment, Biomed Pharmacother, 142 (2021) 112074.
21. A. Rajan, R.J. Kelly, J.B. Trepel, Y.S. Kim, S.V. Alarcon, S. Kummar, M. Gutierrez, S. Crandon, W.M. Zein, L. Jain, B. Mannargudi, W.D. Figg, B.E. Houk, M. Shnaidman, N. Brega, G. Giaccone, A phase I study of PF-04929113 (SNX-5422), an orally bioavailable heat shock protein 90 inhibitor, in patients with refractory solid tumor malignancies and lymphomas, Clin Cancer Res, 17 (2011) 6831-6839.
22. V. Tripathi, S. Darnauer, N.R. Hartwig, W.M. Obermann, Aha1 can act as an autonomous chaperone to prevent aggregation of stressed proteins, J Biol Chem, 289 (2014) 36220-36228.
23. A. Dongre, R.A. Weinberg, New insights into the mechanisms of epithelial-mesenchymal transition and implications for cancer, Nat Rev Mol Cell Biol, 20 (2019) 69-84.
24. T. Mayanagi, T. Morita, K. Hayashi, K. Fukumoto, K. Sobue, Glucocorticoid receptor-mediated expression of caldesmon regulates cell migration via the reorganization of the actin cytoskeleton, J Biol Chem, 283 (2008) 31183-31196.
25. J.J. Lin, Y. Li, R.D. Eppinga, Q. Wang, J.P. Jin, Chapter 1: roles of caldesmon in cell motility and actin cytoskeleton remodeling, Int Rev Cell Mol Biol, 274 (2009) 1-68.
26. S. Dierks, S. von Hardenberg, T. Schmidt, F. Bremmer, P. Burfeind, S. Kaulfuß, Leupaxin stimulates adhesion and migration of prostate cancer cells through modulation of the phosphorylation status of the actin-binding protein caldesmon, Oncotarget, 6 (2015) 13591-13606.
27. Q. Hou, H.T. Tan, K.H. Lim, T.K. Lim, A. Khoo, I.B. Tan, K.G. Yeoh, M.C. Chung, Identification and functional validation of caldesmon as a potential gastric cancer metastasis-associated protein, J Proteome Res, 12 (2013) 980-990.
28. S.J. Moschos, R.J. Sullivan, W.J. Hwu, R.K. Ramanathan, A.A. Adjei, P.C. Fong, R. Shapira-Frommer, H.A. Tawbi, J. Rubino, T.S. Rush, 3rd, D. Zhang, N.R. Miselis, A.A. Samatar, P. Chun, E.H. Rubin, J. Schiller, B.J. Long, P. Dayananth, D. Carr, P. Kirschmeier, W.R. Bishop, Y. Deng, A. Cooper, G.W. Shipps, B.H. Moreno, L. Robert, A. Ribas, K.T. Flaherty, Development of MK-8353, an orally administered ERK1/2 inhibitor, in patients with advanced solid tumors, JCI Insight, 3 (2018).

Figures

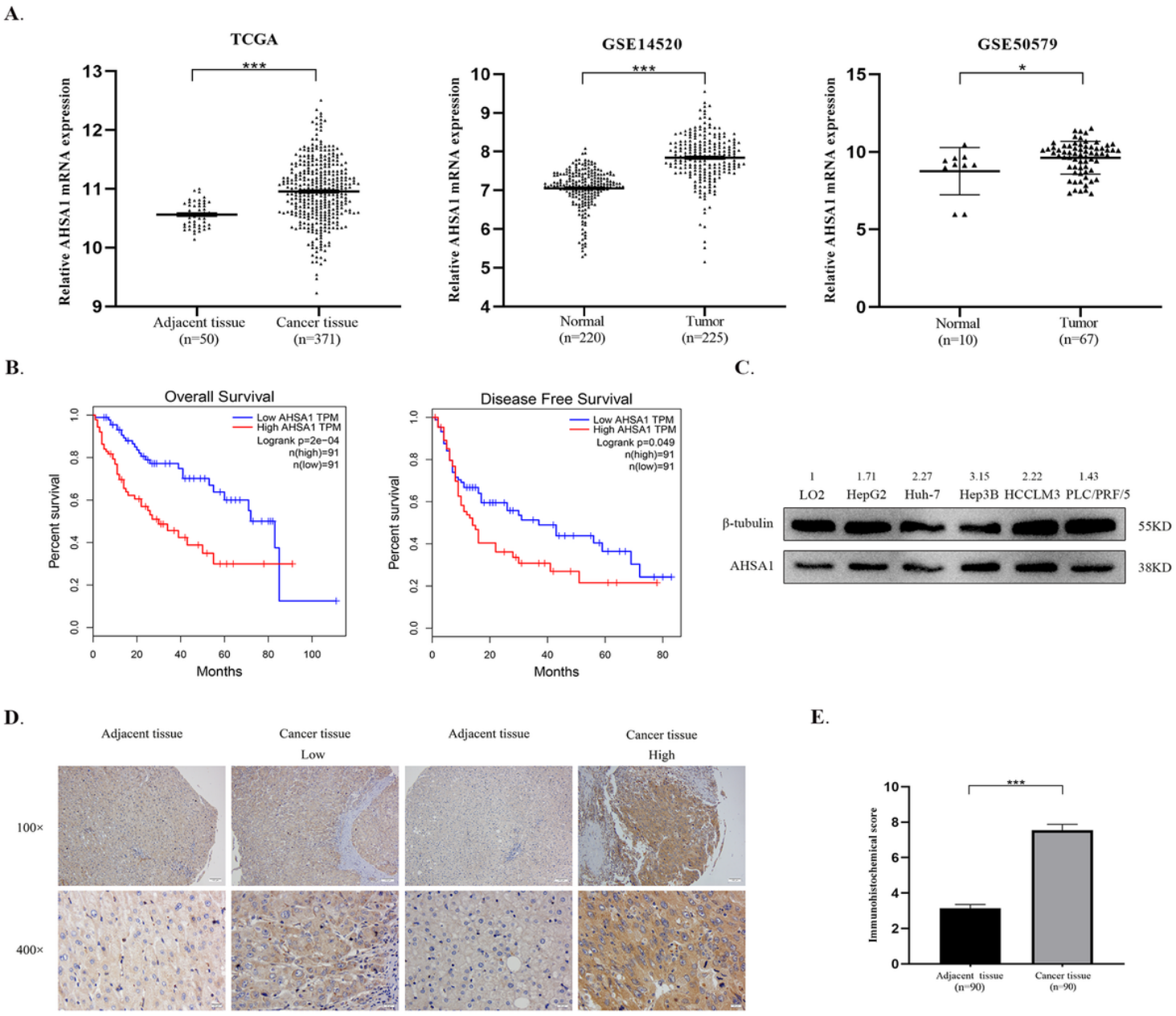

Figure 1

AHSA1 was upregulated and predicted a poor prognosis of HCC

A. AHSA1 was significantly upregulated in HCC cancerous tissues compared with adjacent normal liver tissues. B. HCC patients with high-expression of AHSA1 had shorter OS and DFS than those with low-expression of AHSA1. C. Protein expression of AHSA1 in five common HCC cells and one normal immortalized hepatic epithelial cell (LO2). D and E. Representative IHC images and IHC scores of AHSA1 expression in HCC cancer and adjacent tissues of 90 HCC patients. *, P<0.05; ***, P < 0.001.

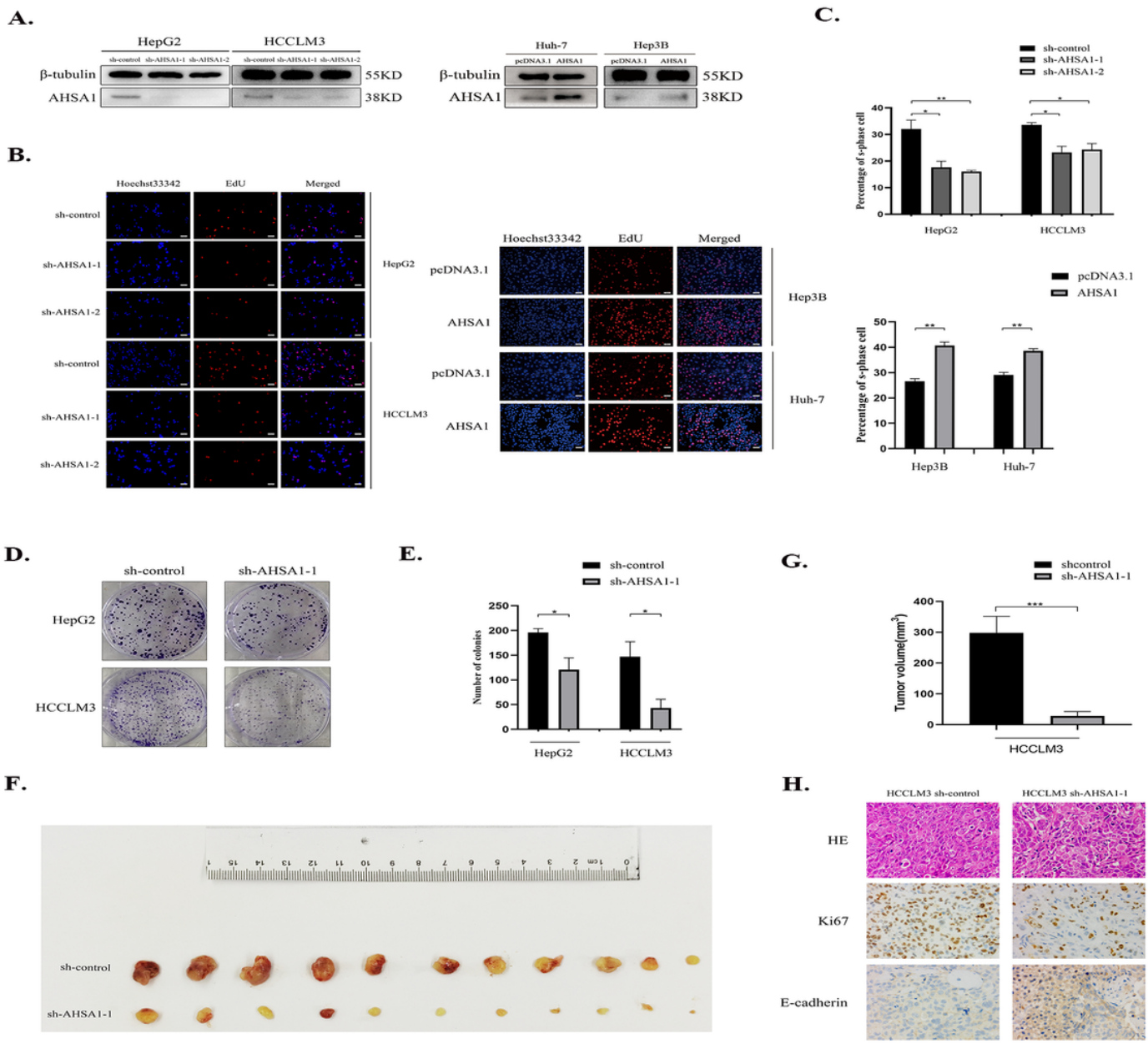

Figure 2

AHSA1 promoted the proliferation of HCC both in vitro and in vivo

A. Transfection efficiency was determined by Western blotting in indicated HCC cell lines. B and C. EdU detection and corresponding statistical analysis were performed on HCC cells. D and E. Cell cloning and statistical analysis were performed on HCC cells after knocking down AHSA1. F and G. Subcutaneous tumor and statistical analysis of tumor volume of HCCLM3-con and HCCLM3-shAHSA1 cells in nude mice. H. HE and IHC staining of Ki-67 and E-cadherin in subcutaneous tumor tissue. *, P<0.05; **, P < 0.01; ***, P < 0.001.

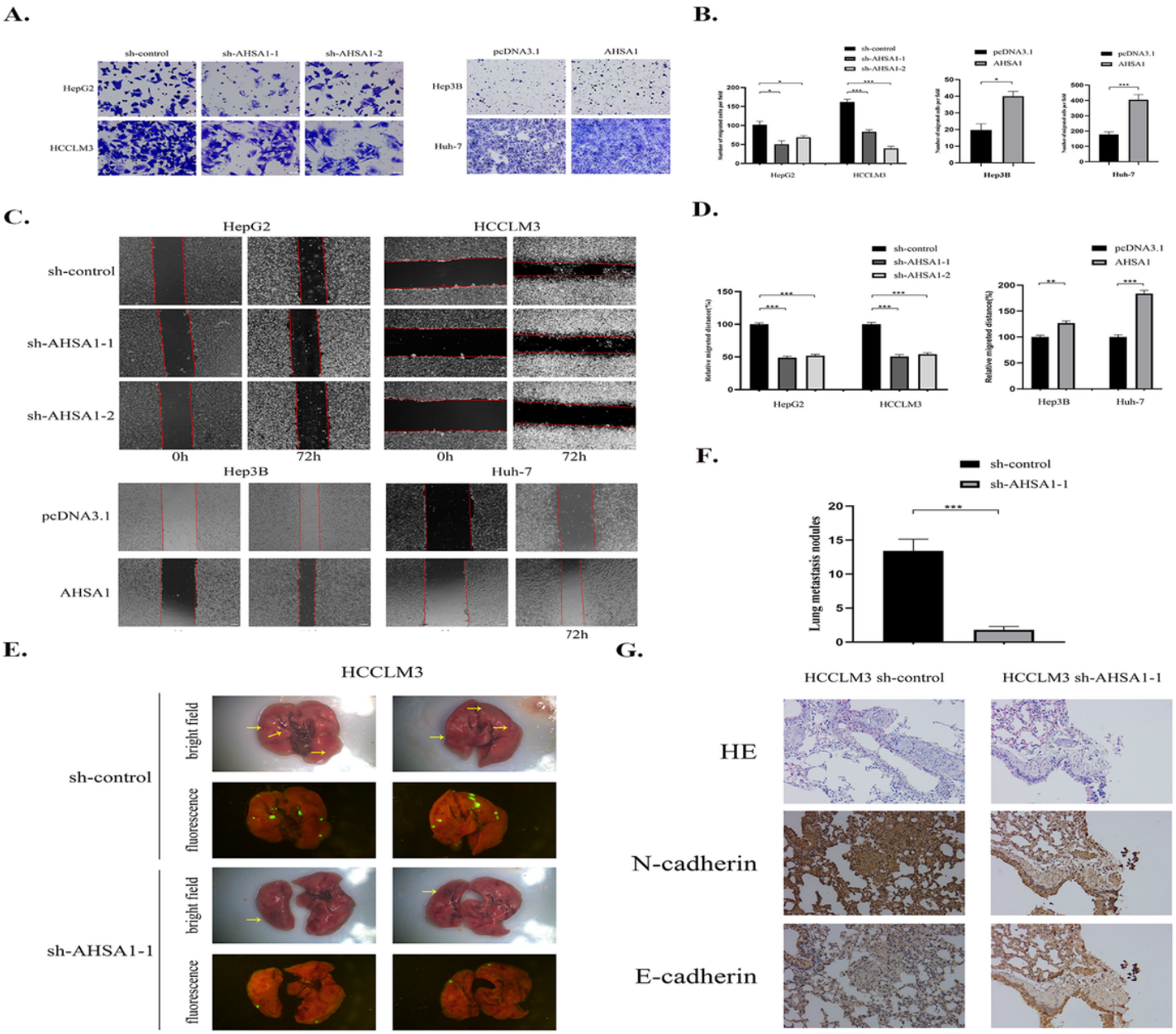

Figure 3

AHSA1 promoted the invasion, migration, and EMT of HCC both in vitro and in vivo

A and B. Representative images and quantitative analysis of Transwell assays in indicated HCC cell lines. C and D. Representative images and the corresponding quantitative analysis of wound healing assays. E and F. Representative images and quantitative analysis of the number of lung metastatic nodules in a nude mouse lung metastasis model by tail vein injection of indicated HCC cells; yellow arrow represents metastasis. G. Representative images of HE and IHC staining of N-cadherin and E-cadherin in lung tissue of nude mice. *, P<0.05; **, P < 0.01; ***, P < 0.001.

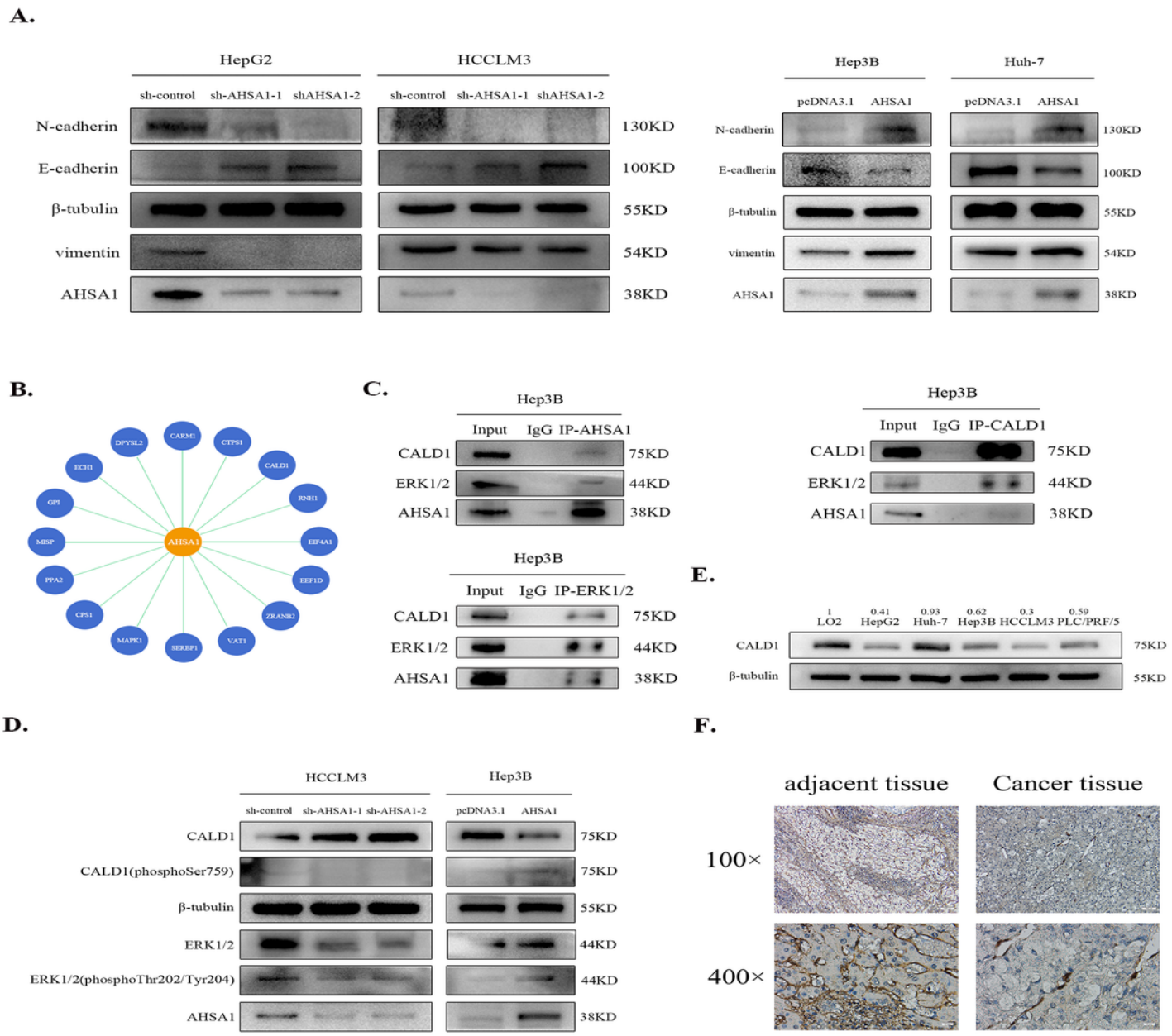

Figure 4

AHSA1 promoted the phosphorylation and inactivation of CALD1 by phosphorylation of ERK1/2

A. EMT markers were analyzed by Western blot by changing AHSA1 expression in HCC cells. B. Proteins that may interact with AHSA1 were obtained by qualitative mass spectrometry. C. AHSA1-ERK1/2-CALD1 was analyzed using Co-IP of the Hep3B cell lysate, and Western blot. D. Protein levels of downstream molecules in HCC cells with AHSA1 knock-down or overexpression were analyzed by Western blot. E. CALD1 protein expression in HCC cells lines and normal immortalized liver epithelial cells were analyzed. F. Representative IHC images of CALD1 expression in cancer and adjacent tissues from HCC patients.

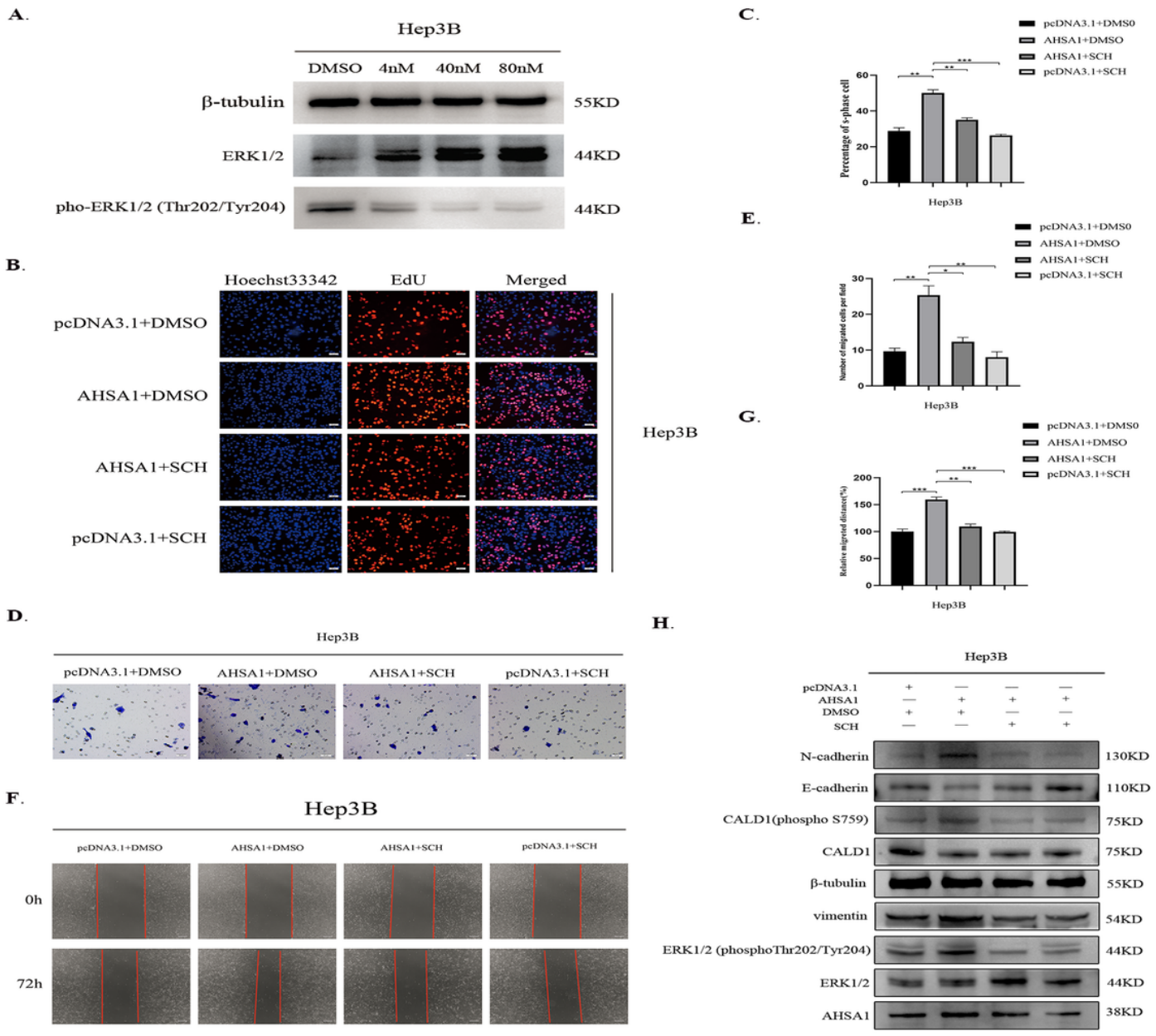

Figure 5

ERK1/2 phosphorylation inhibitor reversed the proliferation and EMT of HCC that was promoted by AHSA1 overexpression.

A. The inhibitory efficiency of different concentrations of SCH772984 on Hep3B cells was analyzed by Western blot. B and C. Representative images and quantitative analysis of EdU staining showed SCH772984 reversed the proliferation induced by overexpression of AHSA1 in Hep3B cells. D-G. Representative images and quantitative analysis of Transwell and wound healing assays showed SCH772984 reversed the migration induced by overexpression of AHSA1 in Hep3B cells. H. The changes in protein expression after inhibiting ERK1/2 phosphorylation in Hep3B cells that overexpressed AHSA1 were detected by Western blot. *, P<0.05; **, P < 0.01; ***, P < 0.001.

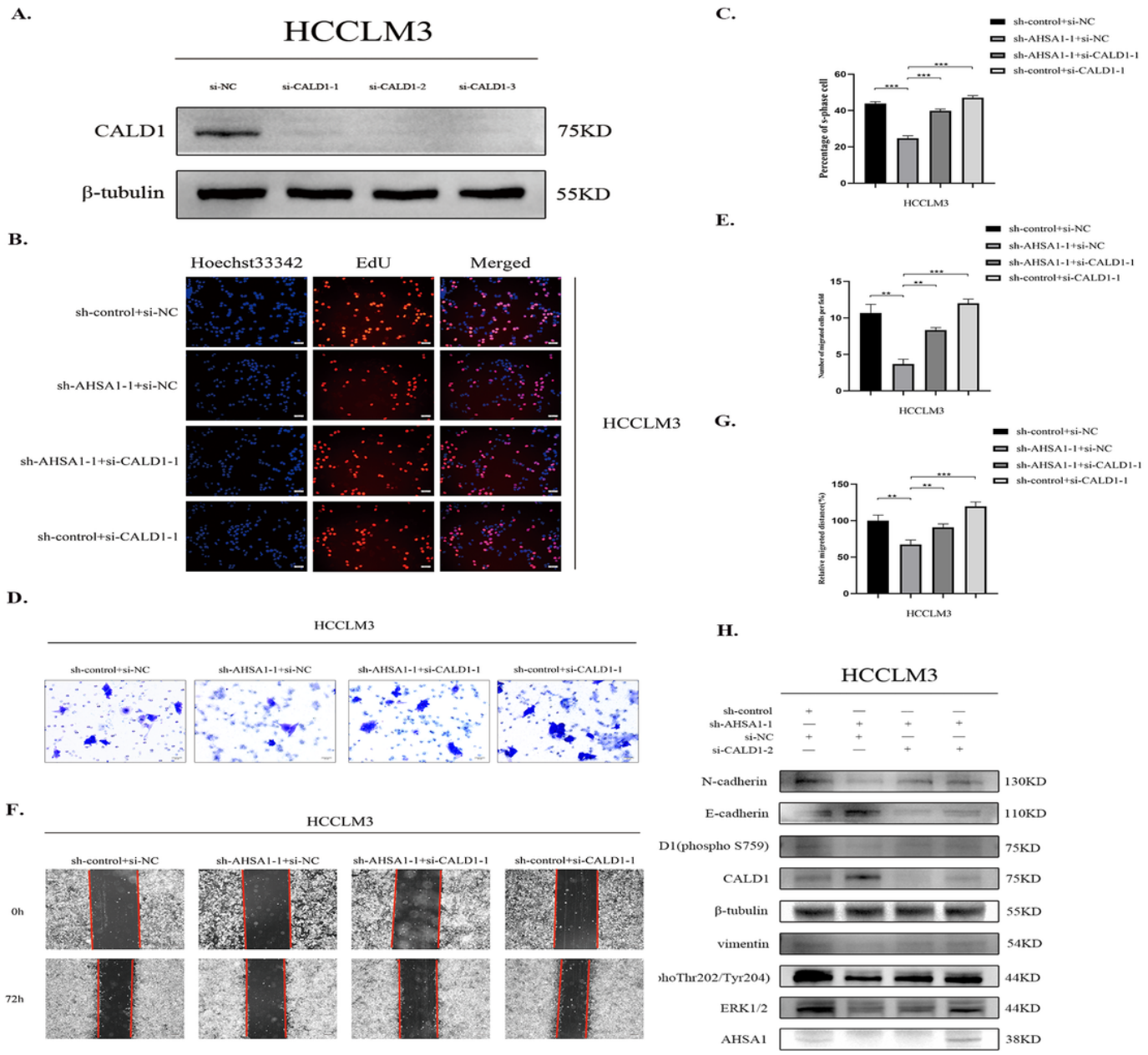

Figure 6

Inhibition of CALD1 reversed the inhibition of cell proliferation and EMT in HCC by knockdown of AHSA1.

A. The efficiency of CALD1 knock-down in HCCLM3 cells was detected by Western blot. B and C. Representative images and quantitative analysis of EdU imaging showed that knockdown of AHSA1 significantly inhibited HCC proliferation which could be reversed by CALD1 silencing. D-G. Representative images and quantitative analysis of Transwell and wound healing assays showed knockdown of AHSA1 led to decreased HCC invasion and migration, which could be reversed by CALD1 silencing. H. The changes in protein expression after inhibiting CALD1 expression in HCCLM3 cells with AHSA1 knock-down were detected by Western blot. **, P < 0.01; ***, P < 0.001.

Supplementary Files

This is a list of supplementary files associated with this preprint. Click to download.

- FigureS1.tif
- FigureS2.tif
- Table.S1.docx